

Weak annihilation and the effective parameters a_1 and a_2 in non-leptonic D decays

H.-Y. Cheng^{1,2}

¹ Institute of Physics, Academia Sinica, Taipei, 115 Taiwan, R.O.C.

² C.N. Yang Institute for Theoretical Physics, State University of New York, Stony Brook, New York 11794, USA

Received: 19 July 2002 /

Published online: 20 November 2002 – © Springer-Verlag / Società Italiana di Fisica 2002

Abstract. Based on SU(3) flavor symmetry, many of the quark-graph amplitudes in two-body non-leptonic decays of charmed mesons can be extracted from experiment, which enable us to see the relevance and importance of weak annihilation topologies and to determine the complex parameters a_1 and a_2 to test the factorization approach. It is found that a_2/a_1 in $D \rightarrow \bar{K}^* \pi$ and $D \rightarrow \bar{K} \rho$ can be different by a factor of 2, indicating that non-factorizable corrections to the latter are far more important than the former. The relative phase between a_1 and a_2 is about 150° . Weak annihilation topologies induced by nearby resonances via final-state rescattering can be described in a model-independent manner. Although the W -exchange contribution in $D \rightarrow PP$ decays is dominated by resonant final-state interactions (FSIs), its amplitude in VP decays (V : vector meson, P : pseudoscalar meson) receives little contributions from FSIs in the quark–antiquark resonance formation. As a consequence, the sign flip of the W -exchange amplitude in $D \rightarrow \bar{K}^* \pi$ and $\bar{K} \rho$ decays, which is needed to explain the relatively real decay amplitudes of $D \rightarrow \bar{K} \rho$, remains unexplained. SU(3) symmetry is badly broken in some Cabibbo-suppressed modes and this can be accounted for by the accumulation of some modest SU(3) violation in individual quark-graph amplitudes.

1 Introduction

The hadronic decays of charmed mesons and related physics have been studied extensively in the past 25 years and a lot of progress has been made. The charm lifetimes, e.g., $\tau(D_s^+)$ and $\tau(\Xi_c^+)$, the D^0 – \bar{D}^0 mixing and the Dalitz plot analyses of three-body charm decays are some of the main topics that are currently being studied. Many new results are expected soon from the dedicated experiments conducted at CLEO, E791, FOCUS, SELEX and the B factories BaBar and Belle.

Contrary to the experimental progress, the theoretical advancement is relatively slow. It is known that the conventional naive factorization approach fails to describe color-suppressed (class-II) decay modes. Empirically, it was learned in the 1980s that if the Fierz-transformed terms characterized by $1/N_c$ are dropped, the discrepancy between theory and experiment is greatly improved [1]. This leads to the so-called large- N_c approach for describing hadronic D decays [2]. Theoretically, explicit calculations based on the QCD sum-rule analysis [3] indicate that the Fierz terms are indeed largely compensated by the non-factorizable corrections. Due to the success of the $1/N_c$ approach to charmed meson decays, it was widely believed in the eighties that it applies equally well to the weak hadronic decays of bottom mesons. However, a generalization of the large- N_c approach or the sum-rule analysis [4] to hadronic B decays leads to some predictions in contradiction to experiment, namely, the destructive inter-

ference in the class-III modes $B^- \rightarrow D^{0(*)} \pi^-$ is not borne out by the data. In the heavy quark limit, non-factorizable corrections to non-leptonic decays are calculable due to the suppression of power corrections. Unfortunately, the charmed quark is not heavy enough to apply the QCD factorization approach [5] or pQCD in a reliable manner.

Moreover, the importance of weak annihilation contributions, namely, W -exchange and W -annihilation, is controversial. In practical calculations, it is customary to argue that they are negligible based on the helicity suppression argument. Although the observation of $D^0 \rightarrow \bar{K}^0 \phi$ in the mid-1980s seems to give the first clean evidence of W -exchange, it was claimed in [6] that rescattering effects required by unitarity can produce the same reaction even in the absence of the W -exchange process. Then it was shown in [7] that this rescattering diagram belongs to the generic W -exchange topology. It has been stressed in [7] that even in $D \rightarrow \bar{K} \pi$ decays, the W -exchange contribution is sizable.

It has been established some time ago that a least model-independent analysis of heavy meson decays can be carried out in the so-called quark-diagram approach. In this diagrammatic scenario, all two-body non-leptonic weak decays of heavy mesons can be expressed in terms of six distinct quark diagrams [8, 9, 7]:¹ \mathcal{T} , the color-allowed external W -emission tree diagram; \mathcal{C} , the color-suppressed

¹ Historically, the quark-graph amplitudes $\mathcal{T}, \mathcal{C}, \mathcal{E}, \mathcal{A}$ are originally denoted by $\mathcal{A}, \mathcal{B}, \mathcal{C}, \mathcal{D}$, respectively [8, 9, 7]

internal W -emission diagram; \mathcal{E} , the W -exchange diagram; \mathcal{A} , the W -annihilation diagram; \mathcal{P} , the horizontal W -loop diagram; and \mathcal{V} , the vertical W -loop diagram. (The one-gluon exchange approximation of the \mathcal{P} graph is the so-called ‘‘penguin diagram’’.) It should be stressed that these quark diagrams are classified according to the topologies of weak interactions with all strong-interaction effects included and hence they are *not* Feynman graphs. All quark graphs used in this approach are topological and meant to have all the strong interactions included, i.e. gluon lines are included in all possible ways. Therefore, topological graphs can provide information on final-state interactions (FSIs).

Based on SU(3) flavor symmetry, this model-independent analysis enables us to extract the topological quark-graph amplitudes and see the relative importance of different underlying decay mechanisms. The quark-diagram scheme, in addition to being helpful in organizing the theoretical calculations, can be used to analyze the experimental data directly. When enough measurements are made with sufficient accuracy, we can find out the values of each quark-diagram amplitude from experiment and compare to theoretical results, especially checking whether there are any final-state interactions or whether the weak annihilations can be ignored as often asserted in the literature.

Recently, Rosner [10] has determined the diagrammatic amplitudes from the measured Cabibbo-allowed two-body D decays. There are several important observations one can learn from this analysis. First, the weak annihilation (W -exchange or W -annihilation) amplitude is sizable with a large phase relative to the tree amplitude. Second, the three $D \rightarrow \bar{K}\rho$ amplitudes are observed to be relatively real, in sharp contrast to the $\bar{K}\pi$ and $\bar{K}^*\pi$ cases. It was argued in [10] that the W -exchange amplitude has to flip its sign from $\bar{K}^*\pi$ to $\bar{K}\rho$ in order to explain why the three decay amplitudes of $D \rightarrow \bar{K}\rho$ are in phase with one another. Third, the color-suppressed amplitude \mathcal{C} has a non-trivial phase relative to the tree amplitude \mathcal{T} . As we shall see, the appearance of non-trivial relative phases between various quark-graph amplitudes implies the relevance and importance of inelastic final-state interactions.

The purpose of this work is twofold: First, we will utilize the reduced quark-graph amplitudes extracted from the data to determine the complex parameters a_1 and a_2 appearing in the factorization approach. This enables us to test the factorization hypothesis and see how important the non-factorizable correction is. Second, we will study weak annihilations induced from nearby quark-antiquark intermediate states. This allows us to explore the effect of inelastic FSIs and see if the sign of the W -exchange topology in Cabibbo-allowed $D \rightarrow VP$ decays is governed by nearby resonances.

The layout of the present paper is as follows. In Sect. 2 we first discuss the quark-diagram amplitudes and then extract the parameters a_1 and a_2 . The diagrammatic amplitudes for Cabibbo-suppressed decay modes and SU(3) violation are addressed. The weak annihilation induced from final-state rescattering in resonance formation is studied in Sect. 3. Its implication and importance for ex-

plaining some D decay modes are discussed. Section 4 is devoted to exploring the color-suppressed amplitude and its phase. We then compare the present study with B decays in Sect. 5 and give conclusions in Sect. 6.

2 Diagrammatic approach

2.1 Quark-graph amplitudes

Based on SU(3) flavor symmetry, the quark-graph amplitudes for the Cabibbo-allowed decays of charmed mesons are listed in Table 1. (For a complete list of the quark-graph amplitudes for Cabibbo singly and doubly suppressed modes, see [7]).² Note that the selection rule for a vanishing $D_s^+ \rightarrow \pi^+\pi^0$ follows from the isospin transformation properties of the weak Hamiltonian and isospin invariance of strong interactions and hence it is unaffected by SU(3) breaking or final-state interactions [14]. For final states involving η or η' it is more convenient to consider the flavor mixing of η_q and η_s defined by

$$\eta_q = \frac{1}{\sqrt{2}}(u\bar{u} + d\bar{d}), \quad \eta_s = s\bar{s}, \quad (2.1)$$

in analogy to the wave functions of ω and ϕ in ideal mixing. The wave functions of the η and η' are given by

$$\begin{pmatrix} \eta \\ \eta' \end{pmatrix} = \begin{pmatrix} \cos \phi & -\sin \phi \\ \sin \phi & \cos \phi \end{pmatrix} \begin{pmatrix} \eta_q \\ \eta_s \end{pmatrix}, \quad (2.2)$$

where $\phi = \theta + \arctan\sqrt{2}$, and θ is the η - η' mixing angle in the octet-singlet basis

$$\begin{pmatrix} \eta \\ \eta' \end{pmatrix} = \begin{pmatrix} \cos \theta & -\sin \theta \\ \sin \theta & \cos \theta \end{pmatrix} \begin{pmatrix} \eta_8 \\ \eta_0 \end{pmatrix}. \quad (2.3)$$

The $D \rightarrow M\eta$ and $M\eta'$ amplitudes have the expressions

$$\begin{aligned} A(D \rightarrow M\eta) &= A(D \rightarrow M\eta_q) \cos \phi \\ &\quad - A(D \rightarrow M\eta_s) \sin \phi, \\ A(D \rightarrow M\eta') &= A(D \rightarrow M\eta_q) \sin \phi \\ &\quad + A(D \rightarrow M\eta_s) \cos \phi. \end{aligned} \quad (2.4)$$

Note that the $D \rightarrow \bar{K}\pi$ amplitudes satisfy the isospin triangle relation

$$\begin{aligned} A(D^+ \rightarrow \bar{K}^0 \pi^+) \\ = A(D^0 \rightarrow K^- \pi^+) + \sqrt{2}A(D^0 \rightarrow \bar{K}^0 \pi^0) \end{aligned} \quad (2.5)$$

² For charm decays involving an SU(3) singlet in the final product, e.g., $D^0 \rightarrow \bar{K}^0 \phi, \bar{K}^0 \omega, \bar{K}^0 \eta_0$, there exist additional hairpin diagrams in which a quark-antiquark pair is created from vacuum to form a color- and flavor-singlet final-state meson [11, 12]. There are four different types of disconnected hairpin diagrams: $\mathcal{E}_h, \mathcal{A}_h, \mathcal{P}_h, \mathcal{D}_h$ corresponding to the quark graphs $\mathcal{E}, \mathcal{A}, \mathcal{P}, \mathcal{D}$ (for details, see [11]). Here we will omit the contributions from the hairpin diagrams, though they seem to play some role in $D_s^+ \rightarrow \rho^+ \eta'$ [10] and $B \rightarrow K\eta'$ decays [13]

Table 1. Quark-graph amplitudes for Cabibbo-allowed decays of charmed mesons. For the reduced amplitudes \mathcal{T} and \mathcal{C} in the $D \rightarrow VP$ decays, the subscript P (V) implies a pseudoscalar (vector) meson which contains the spectator quark of the charmed meson. For \mathcal{E} and \mathcal{A} amplitudes with the final state $q_1\bar{q}_2$, the subscript P (V) denotes a pseudoscalar (vector) meson which contains the antiquark \bar{q}_2

$D^+ \rightarrow \bar{K}^0 \pi^+$	$\mathcal{T} + \mathcal{C}$	$D^+ \rightarrow \bar{K}^{*0} \pi^+$	$\mathcal{T}_V + \mathcal{C}_P$	$D^+ \rightarrow \bar{K}^0 \rho^+$	$\mathcal{T}_P + \mathcal{C}_V$
$D^0 \rightarrow K^- \pi^+$	$\mathcal{T} + \mathcal{E}$	$D^0 \rightarrow K^{*-} \pi^+$	$\mathcal{T}_V + \mathcal{E}_P$	$D^0 \rightarrow K^- \rho^+$	$\mathcal{T}_P + \mathcal{E}_V$
$\rightarrow \bar{K}^0 \pi^0$	$\frac{1}{\sqrt{2}}(\mathcal{C} - \mathcal{E})$	$\rightarrow \bar{K}^{*0} \pi^0$	$\frac{1}{\sqrt{2}}(\mathcal{C}_P - \mathcal{E}_P)$	$\rightarrow \bar{K}^0 \rho^0$	$\frac{1}{\sqrt{2}}(\mathcal{C}_V - \mathcal{E}_V)$
$\rightarrow \bar{K}^0 \eta_q$	$\frac{1}{\sqrt{2}}(\mathcal{C} + \mathcal{E})$	$\rightarrow \bar{K}^{*0} \eta_q$	$\frac{1}{\sqrt{2}}(\mathcal{C}_P + \mathcal{E}_P)$	$\rightarrow \bar{K}^0 \omega$	$\frac{1}{\sqrt{2}}(\mathcal{C}_V + \mathcal{E}_V)$
$\rightarrow \bar{K}^0 \eta_s$	\mathcal{E}	$\rightarrow \bar{K}^{*0} \eta_s$	\mathcal{E}_V	$\rightarrow \bar{K}^0 \phi$	\mathcal{E}_P
$D_s^+ \rightarrow \bar{K}^0 K^+$	$\mathcal{C} + \mathcal{A}$	$D_s^+ \rightarrow \bar{K}^{*0} K^+$	$\mathcal{C}_P + \mathcal{A}_P$	$D_s^+ \rightarrow \bar{K}^0 K^{*+}$	$\mathcal{C}_V + \mathcal{A}_V$
$\rightarrow \pi^+ \pi^0$	0	$\rightarrow \rho^+ \pi^0$	$\frac{1}{\sqrt{2}}(-\mathcal{A}_P + \mathcal{A}_V)$	$\rightarrow \pi^+ \rho^0$	$\frac{1}{\sqrt{2}}(\mathcal{A}_P - \mathcal{A}_V)$
$\rightarrow \pi^+ \eta_q$	$\sqrt{2}\mathcal{A}$	$\rightarrow \rho^+ \eta_q$	$\frac{1}{\sqrt{2}}(\mathcal{A}_P + \mathcal{A}_V)$	$\rightarrow \pi^+ \omega$	$\frac{1}{\sqrt{2}}(\mathcal{A}_P + \mathcal{A}_V)$
$\rightarrow \pi^+ \eta_s$	\mathcal{T}	$\rightarrow \rho^+ \eta_s$	\mathcal{T}_P	$\rightarrow \pi^+ \phi$	\mathcal{T}_V

and likewise for the $D \rightarrow \bar{K}^* \pi$ and $D \rightarrow \bar{K} \rho$ amplitudes. Now since all three sides of the isospin triangle are measured, we are able to determine the relative phases between the various decay amplitudes. From the measured decay rates [15], we find (only the central values are quoted)

$$\begin{aligned}
 \delta_{D^0 \rightarrow \bar{K}^0 \pi^0, D^0 \rightarrow K^- \pi^+} &= 30^\circ, \\
 \delta_{D^+ \rightarrow \bar{K}^0 \pi^+, D^0 \rightarrow K^- \pi^+} &= 80^\circ, \\
 \delta_{D^0 \rightarrow \bar{K}^{*0} \pi^0, D^0 \rightarrow K^{*-} \pi^+} &= 20^\circ, \\
 \delta_{D^+ \rightarrow \bar{K}^{*0} \pi^+, D^0 \rightarrow K^{*-} \pi^+} &= 97^\circ, \\
 \delta_{D^0 \rightarrow \bar{K}^0 \rho^0, D^0 \rightarrow K^- \rho^+} &\approx 0^\circ, \\
 \delta_{D^+ \rightarrow \bar{K}^0 \rho^+, D^0 \rightarrow K^- \rho^+} &\approx 0^\circ,
 \end{aligned}
 \tag{2.6}$$

where we have used the relation, for example,

$$\begin{aligned}
 &\cos \delta_{\{\bar{K}^0 \pi^0, K^- \pi^+\}} \\
 &= \left\{ \left(\mathcal{B}(D^0 \rightarrow K^- \pi^+) + 2\mathcal{B}(D^0 \rightarrow \bar{K}^0 \pi^0) \right. \right. \\
 &\quad \left. \left. - \frac{\tau(D^0)}{\tau(D^+)} \mathcal{B}(D^+ \rightarrow \bar{K}^0 \pi^+) \right) \right\} / \left(2\sqrt{\mathcal{B}(D^0 \rightarrow K^- \pi^+)} \right. \\
 &\quad \left. \times \sqrt{2\mathcal{B}(D^0 \rightarrow \bar{K}^0 \pi^0)} \right) \tag{2.7}
 \end{aligned}$$

to extract the phases. Therefore, the isospin triangle formed by the $\bar{K} \rho$ amplitudes is dramatically different from the one constructed by $\bar{K} \pi$ or $\bar{K}^* \pi$. This triangle is almost flat with zero area, indicating that the three $\bar{K} \rho$ amplitudes are relatively real. This also can be seen from the isospin analysis:

$$\begin{aligned}
 A(D^0 \rightarrow K^- \pi^+) &= \sqrt{\frac{2}{3}} A_{1/2} + \sqrt{\frac{1}{3}} A_{3/2}, \\
 A(D^0 \rightarrow \bar{K}^0 \pi^0) &= -\sqrt{\frac{1}{3}} A_{1/2} + \sqrt{\frac{2}{3}} A_{3/2}, \\
 A(D^+ \rightarrow \bar{K}^0 \pi^+) &= \sqrt{3} A_{3/2},
 \end{aligned}
 \tag{2.8}$$

Table 2. Isospin amplitudes and phase differences for $D \rightarrow \bar{K} \pi, \bar{K}^* \pi, \bar{K} \rho$ decays

	$D \rightarrow \bar{K} \pi$	$D \rightarrow \bar{K}^* \pi$	$D \rightarrow \bar{K} \rho$
$ A_{1/2}/A_{3/2} $	3.83 ± 0.27	5.61 ± 0.35	3.59 ± 0.69
$ \delta_{1/2} - \delta_{3/2} $	$(90 \pm 6)^\circ$	$(104 \pm 13)^\circ$	$< 27^\circ$

with $A_i = |A_i|e^{i\delta_i}$. It turns out that the isospin phase difference is consistent with zero for $D \rightarrow \bar{K} \rho$ (see Table 2).

The reduced quark-graph amplitudes $\mathcal{T}, \mathcal{C}, \mathcal{E}$ have been extracted from Cabibbo-allowed decays by Rosner [10] with the results³

$$\begin{aligned}
 \mathcal{T} &= 2.69 \times 10^{-6} \text{ GeV}, \\
 \mathcal{C} &= (1.96 \pm 0.14)e^{-i152^\circ} \times 10^{-6} \text{ GeV}, \\
 \mathcal{E} &= (1.60 \pm 0.13)e^{i114^\circ} \times 10^{-6} \text{ GeV}, \\
 \mathcal{A} &= 1.10e^{-i70^\circ} \times 10^{-6} \text{ GeV},
 \end{aligned}
 \tag{2.9}$$

from the $D \rightarrow \bar{K} \pi, \bar{K}^0 \eta, \bar{K}^0 \eta'$ and $D_s^+ \rightarrow \bar{K}^0 K^+, \bar{K}^0 \eta, \bar{K}^0 \eta'$ decays, and

$$\begin{aligned}
 \mathcal{T}_V &= (1.78 \pm 0.22) \times 10^{-6}, \\
 \mathcal{C}_P &= 1.48e^{-i152^\circ} \times 10^{-6}, \\
 \mathcal{E}_P &= (1.39 \pm 0.08)e^{i96^\circ} \times 10^{-6},
 \end{aligned}
 \tag{2.10}$$

from $D \rightarrow \bar{K}^* \pi, \bar{K}^0 \phi$ and $D_s^+ \rightarrow \pi^+ \phi$. Without loss of generality, \mathcal{T} has been chosen to be real. The amplitudes $\mathcal{T}, \mathcal{C}, \mathcal{E}, \mathcal{A}$ have dimensions of energy as they are related to the decay rate via

$$\Gamma(D \rightarrow PP) = \frac{p_c}{8\pi m_D^2} |A|^2,
 \tag{2.11}$$

³ The value of the W -annihilation amplitude \mathcal{A} is slightly different from that given in [10] as we have used the D_s^+ lifetime: $\tau(D_s^+) = (0.496_{-0.009}^{+0.010}) \times 10^{-12} \text{ s}$ [15]. It seems to us that the phase difference $|\delta_{AE}|$ quoted in Table IV of [10] is too large by 10°

with p_c being the c.m. momentum. In contrast, the reduced amplitudes $\mathcal{T}_{P,V}, \mathcal{C}_{P,V}, \mathcal{E}_{P,V}$ are dimensionless as they are extracted from the relation

$$\Gamma(D \rightarrow VP) = \frac{p_c^3}{8\pi m_V^2} |A|^2. \quad (2.12)$$

Note that our convention for the $D \rightarrow VP$ amplitudes is the same as that in [7] but different from those of Rosner [10]; this allows one to compare the theoretical calculations of VP amplitudes directly with the quark-graph amplitudes extracted from experiment. It should be stressed that the solutions given above are not unique. For example, a small \mathcal{T} amplitude with the magnitude of 1.1×10^{-6} GeV is also allowed. However, it is not favored by the factorization approach [10, 7]. The original analysis by Rosner is based on the η - η' mixing angle $\theta = -19.5^\circ$ (or $\phi = 35.2^\circ$) from which the η and η' wave functions have simple expressions [16]:

$$\begin{aligned} \eta &= \frac{1}{\sqrt{3}}(\sqrt{2}\eta_q - \eta_s) = \frac{1}{\sqrt{3}}(u\bar{u} + d\bar{d} - s\bar{s}), \\ \eta' &= \frac{1}{\sqrt{3}}(\eta_q + \sqrt{2}\eta_s) = \frac{1}{\sqrt{6}}(u\bar{u} + d\bar{d} + 2s\bar{s}). \end{aligned} \quad (2.13)$$

From Table 1, it is easily seen that $A(D^0 \rightarrow \bar{K}^0 \eta) = \mathcal{C}/(3^{1/2})$. Hence, the diagrammatic amplitude \mathcal{C} is ready to be determined once this mode is measured. A phenomenological analysis of many different experimental processes indicates $\theta = -15.4^\circ$ or $\phi = 39.3^\circ$ [17]. However, we find that the above diagrammatic amplitudes (2.9) and (2.10) describe the observed rates well.

In order to extract the quark-graph amplitudes $\mathcal{T}_P, \mathcal{C}_V$ and \mathcal{E}_V from $D \rightarrow \bar{K}\rho, \bar{K}^* \eta, \bar{K}^* \eta', \bar{K}^0 \omega$ decays, some assumptions have to be made. As noted in passing, the most prominent feature of the $D \rightarrow \bar{K}\rho$ data is that all their three decay amplitudes are almost in phase with one another. Therefore, the quark-graph amplitudes have to be aligned in such a way as to render the resultant various decay amplitudes of $D \rightarrow \bar{K}\rho$ parallel or antiparallel. There exist three possibilities:

- (i) $\mathcal{T}_P, \mathcal{C}_V$ and \mathcal{E}_V are relatively real,
- (ii) the amplitudes \mathcal{T}_P and \mathcal{C}_V possess a relative phase of order -150° as in $\bar{K}\pi$ and $\bar{K}^* \pi$ cases, but $\mathcal{E}_V \approx -\mathcal{E}_P$, and
- (iii) \mathcal{E}_V is close to \mathcal{E}_P , but the relative phase between \mathcal{C}_V and \mathcal{T}_P changes sign. The first possibility was first pointed out by Close and Lipkin [18]. It turns out that the four data of $D \rightarrow \bar{K}\rho$ and $D^0 \rightarrow \bar{K}^0 \omega$ can be fit by setting the three quark-graph amplitudes to

$$\begin{aligned} \text{(i)} \quad \mathcal{T}_P &= 1.20 \times 10^{-6}, \quad \mathcal{C}_V = 0.21 \times 10^{-6}, \\ \mathcal{E}_V &= 1.56 \times 10^{-6}. \end{aligned} \quad (2.14)$$

As stressed by Close and Lipkin, this fit implies that $\mathcal{E}_V \gtrsim \mathcal{T}_P \gg \mathcal{C}_V$ and that the interference in the decay $D^+ \rightarrow \bar{K}^0 \rho^+$ is constructive, contrary to the case of $D^+ \rightarrow \bar{K}^0 \pi^+$ and $\bar{K}^{*0} \pi^+$. However, this fit will be discarded for the following reason. Since $\mathcal{T}_P < \mathcal{T}_V$ and $\mathcal{C}_V \ll \mathcal{C}_P$, the branching ratios for $D_s^+ \rightarrow \bar{K}^0 K^{*+}$ and $D_s^+ \rightarrow \rho^+(\eta, \eta')$ will

become quite small. Neglecting the W -annihilation amplitudes \mathcal{A}_V and \mathcal{A}_P for the moment, the fit (2.14) leads to the predictions

$$\begin{aligned} \mathcal{B}(D_s^+ \rightarrow \bar{K}^0 K^{*+}) &= 5.3 \times 10^{-4}, \\ \mathcal{B}(D_s^+ \rightarrow \rho^+ \eta) &= 1.1\%, \\ \mathcal{B}(D_s^+ \rightarrow \rho^+ \eta') &= 0.45\%, \end{aligned} \quad (2.15)$$

which are too small compared to the corresponding experimental results [15]: $(4.3 \pm 1.4)\%$, $(10.8 \pm 3.1)\%$, $(10.1 \pm 2.8)\%$. As shown below, \mathcal{A}_P and \mathcal{A}_V are constrained by the measurements of $D_s^+ \rightarrow \pi^+ \rho^0$ and $\pi^+ \omega$ and they are small in magnitude. Within the allowed regions of \mathcal{A}_V and \mathcal{A}_P constrained by (2.17) and (2.18), the predicted branching ratios for the aforementioned three modes are still too small, especially for the $\bar{K}^0 K^{*+}$ decay. For example, it is found that $\mathcal{B}(D_s^+ \rightarrow \bar{K}^0 K^{*+}) = 0.35\%$ for $\mathcal{A}_V = 3.3 \times 10^{-7}$. Fit (i) is also unnatural in the sense that FSIs will generally induce relative phases between various quark-graph amplitudes.

The second scenario is considered by Rosner [10] based on the argument that if the W -exchange amplitude is dominated by quark-antiquark intermediate states, then a sign flip of \mathcal{E}_V relative to \mathcal{E}_P will be a consequence of charge-conjugation invariance. As stressed by Rosner, the presence of large final-state phases in the $\bar{K}\rho$ case is masked by the cancellation between \mathcal{C}_V and \mathcal{E}_V . This accidental cancellation arises in $\bar{K}\rho$ decays but not in $\bar{K}\pi$ and $\bar{K}^* \pi$ decays. In the following we list two other fits for the quark-graph amplitudes of $\mathcal{T}_P, \mathcal{C}_V$ and \mathcal{C}_P :

$$\begin{aligned} \text{(ii)} \quad \mathcal{T}_P &= 2.24 \times 10^{-6}, \\ \mathcal{C}_V &= (1.07 \pm 0.18)e^{-i148^\circ} \times 10^{-6}, \\ \mathcal{E}_V &= 1.20e^{-i72^\circ} \times 10^{-6}, \\ \text{(iii)} \quad \mathcal{T}_P &= 2.24 \times 10^{-6}, \\ \mathcal{C}_V &= (1.07 \pm 0.18)e^{i148^\circ} \times 10^{-6}, \\ \mathcal{E}_V &= 1.20e^{i72^\circ} \times 10^{-6}, \end{aligned} \quad (2.16)$$

where fit (ii) was first obtained by [10]. It is easily seen that although both fits give the same decay rates for $D \rightarrow \bar{K}\rho$, they yield different predictions for $D^0 \rightarrow \bar{K}^{*0} \eta$. For $\phi = 39.3^\circ$, we find $\mathcal{B}(D^0 \rightarrow \bar{K}^{*0} \eta) = 1.5\%$ for fit (ii) and 0.78% for fit (iii), while the experimental branching ratio is $(1.9 \pm 0.5)\%$ [15]. Hence, it appears that fit (ii) for the quark-graph amplitudes is preferred. Moreover, as we shall see in Sect. 4, a model calculation of inelastic final-state rescattering indicates that the imaginary part of the color-suppressed amplitude \mathcal{C}_V is negative, in accord with fit (ii). However, it will be shown later (Sect. 3.3) that the W -exchange amplitudes \mathcal{E}_P and \mathcal{E}_V are not dominated by resonant FSIs and hence the sign flip of \mathcal{E}_V from \mathcal{E}_P remains unexplained. Therefore, fit (iii) for the quark-graph amplitudes \mathcal{C}_V and \mathcal{E}_V is not entirely ruled out. It is worth mentioning that, contrary to fit (i), fit (ii) or (iii) has relatively large tree and color-suppressed amplitudes. As a consequence, the interference occurring in $D^+ \rightarrow \bar{K}^0 \rho^+$ has to be destructive in order to accommodate the data.

For the W -annihilation amplitudes \mathcal{A}_P and \mathcal{A}_V , the measurement of $D_s^+ \rightarrow \pi^+\omega$ [15] leads to

$$|\mathcal{A}_P + \mathcal{A}_V| = (4.5 \pm 1.0) \times 10^{-7}, \quad (2.17)$$

while the amplitude $|\mathcal{A}_P - \mathcal{A}_V|$ can be extracted from the recent E791 experiment [19] $\Gamma(D_s^+ \rightarrow \rho^0\pi^+)/\Gamma(D_s^+ \rightarrow \pi^+\pi^+\pi^-) = (5.8 \pm 2.3 \pm 3.7)\%$, though it does not have enough statistical significance. The result is

$$|\mathcal{A}_P - \mathcal{A}_V| = (2.0 \pm 1.2) \times 10^{-7}, \quad (2.18)$$

where use of $\mathcal{B}(D_s^+ \rightarrow \pi^+\pi^+\pi^-) = (1.0 \pm 0.4)\%$ [15] has been made. It will be shown in Sect. 3.2 that $\mathcal{A}_P - \mathcal{A}_V$ receives dominant contributions from resonance-induced FSI. Equations (2.17) and (2.18) suggest that the phase difference between \mathcal{A}_P and \mathcal{A}_V is less than 90° and that the magnitude of \mathcal{A}_P or \mathcal{A}_V is substantially smaller than \mathcal{E}_P and \mathcal{E}_V , contrary to the PP case. The suppression of W -annihilation will be explained in Sect. 3.

Without W -annihilation, fit (ii) leads to

$$\begin{aligned} \mathcal{B}(D_s^+ \rightarrow \bar{K}^0 K^{*+}) &= 1.4\%, \\ \mathcal{B}(D_s^+ \rightarrow \rho^+\eta) &= 3.9\%, \\ \mathcal{B}(D_s^+ \rightarrow \rho^+\eta') &= 1.6\%. \end{aligned} \quad (2.19)$$

In the presence of W -annihilation contributions, the decay amplitudes of $D_s^+ \rightarrow \rho^+\eta^{(\prime)}$ read [see Table 1 and (2.4)]

$$\begin{aligned} A(D_s^+ \rightarrow \rho^+\eta) &= -\mathcal{T}_P \sin \phi + \frac{1}{\sqrt{2}}(\mathcal{A}_P + \mathcal{A}_V) \cos \phi, \\ A(D_s^+ \rightarrow \rho^+\eta') &= \mathcal{T}_P \cos \phi + \frac{1}{\sqrt{2}}(\mathcal{A}_P + \mathcal{A}_V) \sin \phi. \end{aligned} \quad (2.20)$$

It is obvious that $\rho^+\eta$ and $\rho^+\eta'$ cannot be accommodated simultaneously because if W -annihilation contributes constructively to the former, it will contribute destructively to the latter, and vice versa. This issue has been discussed in [20–23] and it is generally believed that the large discrepancy between theory and experiment means that there is an additional contribution to $\rho^+\eta'$ owing to the special character of the η' . As an illustration, we find

$$\begin{aligned} \mathcal{B}(D_s^+ \rightarrow \bar{K}^0 K^{*+}) &= 2.2\%, \\ \mathcal{B}(D_s^+ \rightarrow \rho^+\eta) &= 5.4\%, \\ \mathcal{B}(D_s^+ \rightarrow \rho^+\eta') &= 1.2\%, \end{aligned} \quad (2.21)$$

for $\mathcal{A}_P + \mathcal{A}_V = -4.5 \times 10^{-7}$ and $\mathcal{A}_V = -3.3 \times 10^{-7}$. The smallness of $\rho^+\eta'$ from tree and W -annihilation contributions may indicate the relevance and importance of the hairpin diagrams for the $\rho^+\eta'$ decay. For example, an enhancement mechanism has been suggested in [21] that a $c\bar{s}$ pair annihilates into a W^+ and two gluons, then the two gluons will hadronize mostly into η' . The other possibility is that the gluonic component of the η' , which can be identified with the physical state, e.g. the gluonium, couples to two gluons directly.

There are several important observations of the above extracted reduced quark-graph amplitudes.

(i) The W -exchange or W -annihilation contribution is in general comparable to the internal W -emission and hence cannot be neglected, as stressed in [7]. The weak annihilation amplitude has a phase of order 90° relative to \mathcal{T} and this is suggestive of the importance of resonant contributions to weak annihilations in D decays.

(ii) The W -annihilation \mathcal{A} and W -exchange amplitudes \mathcal{E} have opposite signs.

(iii) The color-suppressed internal W -emission amplitude \mathcal{C} has a phase $\sim 150^\circ$ relative to \mathcal{T} for all Cabibbo-allowed D decays. In the factorization approach, the relative phase is 180° .

(iv) The W -exchange amplitude in $\bar{K}^*\pi$ and in $\bar{K}^*\rho$ has an opposite sign. As stressed by Rosner, this sign difference is very crucial to explain why the $D \rightarrow \bar{K}^*\rho$ amplitudes are relatively real, but not so for the $D \rightarrow \bar{K}^*\pi$ and $D \rightarrow \bar{K}^*\pi$ decays.

It was conjectured in [10] that

(i) the opposite sign between \mathcal{E}_P and \mathcal{E}_V arises from the fact that they are dominated by the quark–antiquark intermediate states which have equal and opposite couplings to $K^{*-}\pi^+$ and $K^-\rho^+$ by charge-conjugation invariance, and

(ii) the relative phase between \mathcal{C} and \mathcal{T} comes from inelastic final-state rescattering. We will come to these issues in Sects. 3 and 4.

2.2 Parameters a_1 and a_2

In terms of the factorized hadronic matrix elements, one can define a_1 and a_2 by

$$\begin{aligned} \mathcal{T} &= \frac{G_F}{\sqrt{2}} V_{ud} V_{cs}^* a_1 (\bar{K}\pi) f_\pi (m_D^2 - m_K^2) F_0^{DK}(m_\pi^2), \\ \mathcal{C} &= \frac{G_F}{\sqrt{2}} V_{ud} V_{cs}^* a_2 (\bar{K}\pi) f_K (m_D^2 - m_\pi^2) F_0^{D\pi}(m_K^2), \\ \mathcal{T}_V &= \frac{G_F}{\sqrt{2}} V_{ud} V_{cs}^* a_1 (\bar{K}^*\pi) 2f_\pi m_{K^*} A_0^{DK^*}(m_\pi^2), \\ \mathcal{C}_P &= \frac{G_F}{\sqrt{2}} V_{ud} V_{cs}^* a_2 (\bar{K}^*\pi) 2f_{K^*} m_{K^*} F_1^{D\pi}(m_{K^*}^2), \\ \mathcal{T}_P &= \frac{G_F}{\sqrt{2}} V_{ud} V_{cs}^* a_1 (\bar{K}\rho) 2f_\rho m_\rho F_1^{DK}(m_\rho^2), \\ \mathcal{C}_V &= \frac{G_F}{\sqrt{2}} V_{ud} V_{cs}^* a_2 (\bar{K}\rho) 2f_K m_\rho A_0^{D\rho}(m_K^2), \end{aligned} \quad (2.22)$$

where we have followed [24] for the definition of the form factors. Factorization implies a universal, process-independent a_1 and a_2 ; for example, $a_2(\bar{K}\rho) = a_2(\bar{K}^*\pi) = a_2(\bar{K}\pi)$.

In order to extract the values of a_1 and a_2 we consider two distinct form factor models: the Bauer–Stech–Wirbel (BSW) model [24] and the Melikhov–Stech (MS) model [25], both based on the constituent quark picture. For the q^2 dependence, the BSW model adopts the pole dominance assumption:

$$f(q^2) = \frac{f(0)}{(1 - q^2/m_*^2)^n}, \quad (2.23)$$

Table 3. Form factors in BSW and MS models

	$F_0^{DK}(m_\pi^2)$	$F_0^{D\pi}(m_K^2)$	$F_1^{DK}(m_\rho^2)$	$F_1^{D\pi}(m_{K^*}^2)$	$A_0^{DK^*}(m_\pi^2)$	$A_0^{D\rho}(m_K^2)$
BSW	0.76	0.72	1.01	1.07	0.74	0.77
MS	0.78	0.71	0.93	0.91	0.76	0.73

Table 4. The parameters a_1 and a_2 extracted using the BSW model (first entry) and the MS model (second entry) for form factors. Only the central values for the magnitude and the phase angle are quoted. To see the sensitivity of a_2/a_1 to the W -exchange contribution, its value in the absence of \mathcal{E} is also shown in the last two rows

	$D \rightarrow \bar{K}\pi$	$D \rightarrow \bar{K}^*\pi$	$D \rightarrow \bar{K}\rho$
$ a_1 $	1.02	1.23	0.92
	1.05	1.28	0.85
$ a_2 $	0.63	0.53	0.76
	0.62	0.45	0.72
a_2/a_1	0.62exp(-i152°)	0.43exp(-i152°)	0.82exp(-i148°)
	0.60exp(-i152°)	0.35exp(-i152°)	0.85exp(-i148°)
a_2/a_1 (with $\mathcal{E} = 0$)	0.88exp(-i149°)	0.56exp(-i160°)	-0.87
	0.86exp(-i149°)	0.46exp(-i160°)	-0.90

with m_* being the pole mass. The original BSW model assumes a monopole behavior (i.e. $n = 1$) for all the form factors. However, this is not consistent with heavy quark symmetry scaling relations for heavy-to-light transitions. The modified BSW model takes the BSW model results for the form factors at zero momentum transfer but makes a different ansatz for their q^2 dependence, namely, a dipole behavior (i.e. $n = 2$) is assumed for the form factors F_1, A_0, A_2, V , motivated by heavy quark symmetry, and a monopole dependence for F_0, A_1 . The experimental value of $F_0^{DK}(0)$ is about 0.76 [26], but it is far less certain for $F_0^{D\pi}(0)$. A sum-rule analysis [27] and in particular a recent lattice calculation [28] all give $F_0^{DK}(0)/F_0^{D\pi}(0) \approx 1.20$, in agreement with the results of the BSW and MS models (see Table 3).

The values of a_1 and a_2 and their ratio are listed in Table 4. We see that the ratio of a_2/a_1 is channel dependent; especially its magnitude in $\bar{K}^*\pi$ and $\bar{K}\rho$ decays can be different by a factor of 2. However, its phase of order 150° is essentially process independent. To see the sensitivity of a_2/a_1 to the W -exchange contribution, we set $\mathcal{E} = 0$ and determine a_2/a_1 from the isospin analysis of $D \rightarrow \bar{K}^{(*)}\pi(\rho)$ decays. For example, for $D \rightarrow \bar{K}\pi$ decays we have [29]

$$\frac{a_2}{a_1} \Big|_{D \rightarrow \bar{K}\pi} = \frac{2 - \sqrt{2} \frac{A_{1/2}}{A_{3/2}} \Big|_{D \rightarrow \bar{K}\pi} f_\pi \frac{m_D^2 - m_K^2}{f_K \frac{m_D^2 - m_\pi^2}{F_0^{D\pi}(m_K^2)}} F_0^{DK}(m_\pi^2)}{1 + \sqrt{2} \frac{A_{1/2}}{A_{3/2}} \Big|_{D \rightarrow \bar{K}\pi}} \quad (2.24)$$

The results are shown in the last two rows of Table 4. It is interesting to see that for $\bar{K}\pi$ and $\bar{K}^*\pi$ decays, the phase

of a_2/a_1 is about the same as before, but the magnitude differs slightly, whereas for the $\bar{K}\rho$ system, the magnitude is close to the realistic one, but the phase is different. This is understandable because the three $\bar{K}\rho$ amplitudes are in phase with one another. Hence, a_2/a_1 is real in the absence of the weak annihilation.

What is the relation between the coefficients a_i and the Wilson coefficients in the effective Hamiltonian approach? Under the naive factorization hypothesis, one has

$$\begin{aligned} a_1(\mu) &= c_1(\mu) + \frac{1}{N_c} c_2(\mu), \\ a_2(\mu) &= c_2(\mu) + \frac{1}{N_c} c_1(\mu), \end{aligned} \quad (2.25)$$

for decay amplitudes induced by current-current operators $O_{1,2}(\mu)$, where $c_{1,2}(\mu)$ are the corresponding Wilson coefficients and N_c is the number of colors. In the absence of QCD corrections, $c_1 = 1$ and $c_2 = 0$, and hence class-II modes governed by $a_2 = 1/N_c$ are obviously “color-suppressed”. However, this naive factorization approach encounters two principal difficulties:

- (i) the coefficients a_i given by (2.25) are renormalization scale and γ_5 -scheme dependent, and
- (ii) it fails to describe the color-suppressed class-II decay modes due to the smallness of a_2 . Therefore, it is necessary to take into account non-factorizable corrections:

$$\begin{aligned} a_1 &= c_1(\mu) + c_2(\mu) \left(\frac{1}{N_c} + \chi_1(\mu) \right), \\ a_2 &= c_2(\mu) + c_1(\mu) \left(\frac{1}{N_c} + \chi_2(\mu) \right), \end{aligned} \quad (2.26)$$

where non-factorizable terms are characterized by the parameters χ_i , which receive corrections including vertex

Table 5. Predicted branching ratios of some Cabibbo-suppressed D decays without and with SU(3) violation (denoted by the subscripts “theory1” and “theory2”, respectively) and comparison with experiment. The amplitude \mathcal{E}_q in $D^0 \rightarrow K^0 \bar{K}^0$ decay denotes the $q\bar{q}$ -popping W -exchange amplitude

Decay mode	Amplitude	$\mathcal{B}_{\text{theory1}}$	$\mathcal{B}_{\text{theory2}}$	$\mathcal{B}_{\text{expt}}$ [15]
$D^+ \rightarrow \pi^+ \pi^0$	$\frac{1}{\sqrt{2}} \frac{V_{cd}}{V_{cs}} (\mathcal{T} + \mathcal{C})_{\pi\pi}$	7.6×10^{-4}	2.4×10^{-3}	$(2.5 \pm 0.7) \times 10^{-3}$
$D^0 \rightarrow \pi^+ \pi^-$	$\frac{V_{cd}}{V_{cs}} (\mathcal{T} + \mathcal{E})_{\pi\pi}$	2.1×10^{-3}	1.7×10^{-3}	$(1.52 \pm 0.09) \times 10^{-3}$
$\rightarrow \pi^0 \pi^0$	$\frac{\sqrt{2}}{2} \frac{V_{cd}}{V_{cs}} (\mathcal{C} - \mathcal{E})_{\pi\pi}$	1.2×10^{-3}	0.9×10^{-3}	$(8.4 \pm 2.2) \times 10^{-4}$
$D^+ \rightarrow K^+ \bar{K}^0$	$\frac{V_{us}}{V_{ud}} (\mathcal{T} - \mathcal{A})_{KK}$	4.7×10^{-3}	7.4×10^{-3}	$(7.4 \pm 1.0) \times 10^{-3}$
$D^0 \rightarrow K^+ K^-$	$\frac{V_{us}}{V_{ud}} (\mathcal{T} + \mathcal{E})_{KK}$	1.8×10^{-3}	4.2×10^{-3}	$(4.25 \pm 0.16) \times 10^{-3}$
$\rightarrow K^0 \bar{K}^0$	$\frac{V_{us}}{V_{ud}} (\mathcal{E}_s - \mathcal{E}_d)_{KK}$	–	–	$(6.5 \pm 1.8) \times 10^{-4}$

corrections, hard spectator interactions involving the spectator quark of the heavy meson, and FSI effects from inelastic rescattering, resonance effects, etc. The non-factorizable terms $\chi_i(\mu)$ will compensate the scale and scheme dependence of the Wilson coefficients to render a_i physical. Using the leading order Wilson coefficients $c_1(\bar{m}_c) = 1.274$ and $c_2(\bar{m}_c) = -0.529$ [30] for $\Lambda_{\overline{\text{MS}}} = 215 \text{ MeV}$, where $\bar{m}_c(m_c) \approx 1.3 \text{ GeV}$, it is clear that a_2 is rather sensitive to χ_2 and that the non-factorizable correction to a_2 in the $\bar{K}\rho$ system is far more important than that in $\bar{K}^* \pi$ decays.

Empirically, it was found that the discrepancy between theory and experiment for charm decays is greatly improved if Fierz-transformed terms in (2.25) are dropped [1]. It has been argued that this empirical observation is justified in the so-called large- N_c approach in which a rule of discarding subleading $1/N_c$ terms can be formulated [2]. This amounts to having universal non-factorizable terms $\chi_1 = \chi_2 = -1/N_c$ in (2.26) and hence

$$a_1 = c_1(\bar{m}_c) \approx 1.27, \quad a_2 = c_2(\bar{m}_c) \approx -0.53. \quad (2.27)$$

This corresponds to a relative phase of 180° . From Table 4 we see that the above values of a_1 and a_2 give a good description of the $D \rightarrow \bar{K}^* \pi$ decays and differ not too much from those values for $\bar{K} \pi$ and $\bar{K} \rho$ systems. Hence, a_1 and a_2 in the large- N_c approach can be considered as the benchmarked values. In the heavy quark limit, non-factorizable terms χ_i are calculable due to the suppression of power corrections provided that the emitted meson is light, while the recoiled meson can be either light or heavy [5]. In the QCD factorization approach, the χ_i are found to be positive for B decays [5]. This means that the empiric large- N_c approach cannot be generalized to the B system. For charm decays, the charmed quark is not heavy enough to apply the QCD factorization approach or pQCD in a reliable manner. To our knowledge, the sum-rule approach is more suitable for studying the non-factorized effects in hadronic D decay [3].

2.3 Cabibbo-suppressed modes and SU(3) breaking

So far the diagrammatic amplitudes are determined for Cabibbo-allowed D decays. When generalized to Cabibbo-suppressed modes, there exist some sizable SU(3) breaking effects which cannot be ignored. Table 5 shows the predicted branching ratios (see column 3 denoted by $\mathcal{B}_{\text{theory1}}$) for some of the Cabibbo-suppressed modes using the reduced amplitudes determined from Cabibbo-allowed decays. By comparing with experiment, we see some large discrepancies. To be specific, we consider the ratios

$$R_1 = 2 \left| \frac{V_{cs}}{V_{cd}} \right|^2 \frac{\Gamma(D^+ \rightarrow \pi^0 \pi^+)}{\Gamma(D^+ \rightarrow \bar{K}^0 \pi^+)}, \quad (2.28)$$

$$R_2 = \frac{\Gamma(D^0 \rightarrow K^+ K^-)}{\Gamma(D^0 \rightarrow \pi^+ \pi^-)}.$$

In the SU(3) limit, $R_1 = R_2 = 1$, while the experimental measurements $R_1 = 3.39 \pm 0.70$ and $R_2 = 2.80 \pm 0.20$ [15] show a large deviation from SU(3) flavor symmetry.

As first stressed in [31], model predictions are very difficult to accommodate the measured value of R_1 . It was originally argued in the same reference that the large SU(3) violation manifest in R_1 can be accounted for by the accumulations of several small SU(3) breaking effects, provided that $F_0^{D\pi}(0) > F_0^{DK}(0)$. However, a smaller $F_0^{D\pi}(0)$ is preferred on theoretical grounds, as discussed before. To accommodate the data of $\pi^+ \pi^0$, it is clear that one needs $\mathcal{T}_{\pi\pi} > \mathcal{T}$ and $|\mathcal{C}_{\pi\pi}| < |\mathcal{C}|$. Allowing a modest SU(3) violation in the individual quark-graph amplitudes,

$$\begin{aligned} \mathcal{T}_{\pi\pi} &= 1.25 \mathcal{T}, \\ \mathcal{C}_{\pi\pi} &= 1.6 e^{-i140^\circ} \times 10^{-6} \text{ GeV}, \\ \mathcal{E}_{\pi\pi} &= 1.9 e^{i140^\circ} \times 10^{-6} \text{ GeV}, \end{aligned} \quad (2.29)$$

the data of $D \rightarrow \pi\pi$ are well accounted for (see Table 5). However, we would like to stress that we do not claim that (2.29) is *the* solution for Cabibbo-suppressed $D \rightarrow \pi\pi$ decays; we simply wish to illustrate that a *modest* SU(3) violation in each quark-graph amplitudes can lead to a *large* SU(3) breaking effect for R_1 . In the factorization approach, however, it is difficult to understand why $\mathcal{T}_{\pi\pi} > \mathcal{T}$.

The ratio of K^+K^- to $\pi^+\pi^-$ is a long-standing puzzle. The conventional factorization approach leads to $R_2 \approx 1$ when weak annihilation contributions are neglected. In the diagrammatical approach, it is found that R_2 can be accommodated by allowing SU(3) violation in the tree and W -exchange amplitudes:

$$\begin{aligned}\mathcal{T}_{KK} &= 1.25\mathcal{T}, \\ \mathcal{E}_{KK} &= 1.7e^{i90^\circ} \times 10^{-6} \text{ GeV}, \\ \mathcal{A}_{KK} &= \mathcal{A}.\end{aligned}\quad (2.30)$$

It is known that in the limit of SU(3) symmetry, $D^0 \rightarrow K^0\bar{K}^0$ vanishes. This decay receives contributions from inelastic final-state scattering in analogy to Fig. 1a and it has been discussed recently in [32,33].

3 Weak annihilations and resonant final-state interactions

We learned from Sect. 2 some important information about the weak annihilation topologies \mathcal{E} and \mathcal{A} :

(i) Their contributions are in general comparable to the internal W -emission topological amplitude and they have a phase of order 90° relative to \mathcal{T} with an opposite sign between \mathcal{E} and \mathcal{A} .

(ii) A sign flip of the W -exchange amplitude may occur in $\bar{K}^*\pi$ and $\bar{K}\rho$ decays and this is very crucial for explaining why the $D \rightarrow \bar{K}\rho$ amplitudes are in phase with one another, but not for $D \rightarrow \bar{K}^*\pi$ and $D \rightarrow \bar{K}\pi$ decays. The purpose of this section is to explore these two features.

Under the factorization hypothesis, the factorizable W -exchange and W -annihilation amplitudes are proportional to a_2 and a_1 , respectively. They are suppressed due to the smallness of the form factor $F_0^{0 \rightarrow \bar{K}\pi}(m_D^2)$ at large $q^2 = m_D^2$. This corresponds to the so-called helicity suppression. At first glance, it appears that the factorizable weak annihilation amplitudes are too small to be consistent with experiment at all. However, in the diagrammatic approach here, the topological amplitudes \mathcal{C} , \mathcal{E} , \mathcal{A} can receive contributions from the tree amplitude \mathcal{T} via final-state rescattering, as illustrated in Fig. 1 for $D^0 \rightarrow \bar{K}^0\pi^0$ decay: Fig. 1a has the same topology as W -exchange,⁴ while Fig. 1b mimics the internal W -emission amplitude \mathcal{C} . Therefore, even if the short-distance W -exchange vanishes, a long-distance W -exchange can be induced via inelastic FSIs [34,35]. Historically, it was first pointed out in [6] that rescattering effects required by unitarity can produce the reaction $D^0 \rightarrow \bar{K}^0\phi$, for example, even in the absence of a W -exchange diagram. Then it was shown in [7] that this rescattering diagram belongs to the generic W -exchange topology.

There are several different forms of FSIs: elastic scattering and inelastic scattering such as quark exchange,

⁴ It is also pointed out by Close and Lipkin [18] that the prominent weak annihilation may be largely due to final-state resonance scattering

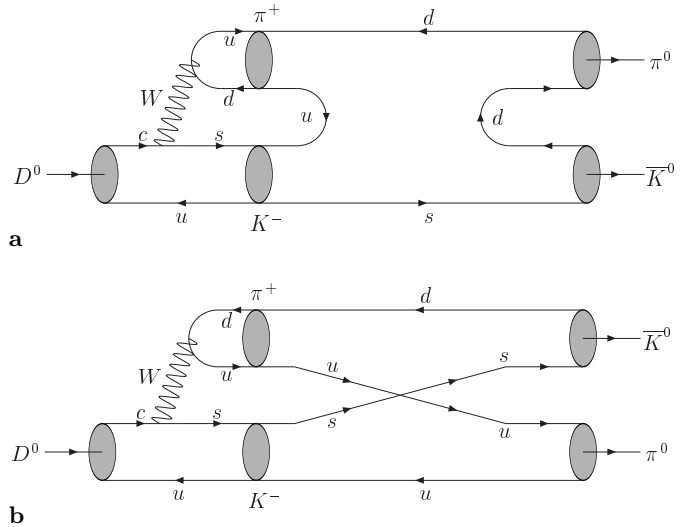


Fig. 1a,b. Contributions to $D^0 \rightarrow \bar{K}^0\pi^0$ from the color-allowed rescattering **a** and quark exchange **b**. While **a** has the same topology as the W -exchange graph, **b** mimics the color-suppressed internal W -emission graph

resonance formation, etc. As emphasized in [34], the resonance formation of FSI via $q\bar{q}$ resonances is probably the most important one. Indeed, there are two indications about the importance of resonant FSIs for weak annihilation topologies: First, the sizable magnitude of \mathcal{E} and \mathcal{A} and their large phases are suggestive of nearby resonance effects. Second, an abundant spectrum of resonances is known to exist at energies close to the mass of the charmed meson.

Since FSIs are non-perturbative in nature, in principle it is notoriously difficult to calculate their effects. It is customary to evaluate the long-distance W -exchange contribution, Fig. 1a, at the hadron level manifested as Fig. 2 [32,36–38]. Take $D^0 \rightarrow \bar{K}^0\pi^0$ as an illustration. Figure 2a shows the resonant amplitude coming from $D^0 \rightarrow K^-\pi^+$ followed by a s -channel $J^P = 0^+$ particle exchange with the quark content $(s\bar{d})$, for example $K_0^*(1950)$, which couples to $\bar{K}^0\pi^0$ and $K^-\pi^+$. Figure 2b corresponds to the t -channel contribution with one-particle exchange. As discussed before, it is expected that the long-distance W -exchange is dominated by resonant FSIs as shown in Fig. 2a. However, a direct calculation of this diagram is subject to many theoretical uncertainties. For example, the coupling of the resonance to $\bar{K}\pi$ states is unknown and the off-shell effects in the chiral loop should be properly addressed [36]. Nevertheless, as pointed out in [34,39], most of the properties of resonances follow from unitarity alone, without regard to the dynamical mechanism that produces the resonance. Consequently, as we shall see below, the effect of resonance-induced FSIs [Fig. 2a] can be described in a model-independent manner in terms of the mass and width of the nearby resonances.

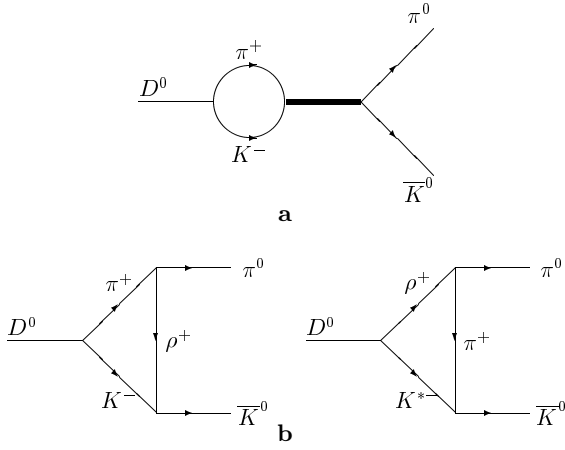


Fig. 2a,b. Manifestation of Fig. 1a as the long-distance s - and t -channel contributions to the W -exchange amplitude in $D^0 \rightarrow \bar{K}^0 \pi^0$. The thick line in **a** represents a resonance

3.1 Formalism

In the presence of resonances, the decay amplitude of the charmed meson D decaying into two mesons $M_1 M_2$ is modified by rescattering through a multiplet of resonances [39]⁵

$$A(D \rightarrow M_i M_j)_{\text{resonant-FSI}} = A(D \rightarrow M_i M_j) - i \frac{\Gamma}{E - m_R + i\Gamma/2} \sum_r c_{ij}^{(r)} \sum_{kl} c_{kl}^{(r)*} A(D \rightarrow M_k M_l), \quad (3.1)$$

where the summation runs over various mass degenerated resonances with the same values of the resonance mass m_R and width Γ , and $c_{ij}^{(r)}$ are the normalized coupling constants of $M_i M_j$ with the resonance r , obeying the orthonormal relations

$$\sum_{ij} c_{ij}^{(r)} c_{ij}^{(s)*} = \delta_{rs}, \quad \sum_{ij} |c_{ij}^{(r)}|^2 = 1. \quad (3.2)$$

The presence of a resonance shows itself in a characteristic behavior of the phase shifts near the resonance. For each individual resonant state r , there is an eigenstate of $A(D \rightarrow M_i M_j)$ with eigenvalue [39]

$$e^{2i\delta_r} = 1 - i \frac{\Gamma}{m_D - m_R + i\Gamma/2}, \quad (3.3)$$

or

$$\tan \delta_r = \frac{\Gamma}{2(m_D - m_R)} \quad (3.4)$$

in the rest frame of the charmed meson. Therefore, resonance-induced coupled-channel effects are amenable technically in terms of the physical resonances.

To illustrate the effect of FSIs in the resonance formation, consider the decays $D^0 \rightarrow \bar{K}_i P_j$ as an example.

⁵ The same expression for (3.1) is also given in [20] except that the phase in (3.3) of [20] is too small by a factor of 2

The only nearby 0^+ scalar resonance with the $(s\bar{d})$ quark content in the charm mass region is $r = K_0^*(1950)$ and the states $\bar{K}_i P_j$ are $K^- \pi^+$, $\bar{K}^0 \pi^0$, $\bar{K}^0 \eta$, $\bar{K}^0 \eta'$. The quark-diagram amplitudes for $D^0 \rightarrow K^- \pi^+$, $\bar{K}^0 \pi^0$, $\bar{K}^0 \eta_q$ and $\bar{K}^0 \eta_s$ are shown in Table 1. It is convenient to decompose $D \rightarrow \bar{K} \pi$ amplitudes into their isospin amplitudes (see (2.8) and Table 1):

$$A(D^0 \rightarrow (\bar{K}\pi)_{3/2}) = \frac{1}{\sqrt{3}}(\mathcal{T} + \mathcal{E}),$$

$$A(D^0 \rightarrow (\bar{K}\pi)_{1/2}) = \frac{1}{\sqrt{6}}(2\mathcal{T} - \mathcal{C} + 3\mathcal{E}), \quad (3.5)$$

where the subscripts 1/2 and 3/2 denote the isospin of the $\bar{K}\pi$ system. Consider the D -type coupling for the strong interaction $P_1 P_2 \rightarrow P'$ (P' : scalar meson), namely $\kappa \text{Tr}(P' \{P_1, P_2\})$ with κ being a flavor-symmetric strong coupling [34]. Noting that $(\bar{K}\pi)_{3/2}$ does not couple to $(\bar{K}\pi)_{1/2}$, $\bar{K}^0 \eta_q$, and $\bar{K}^0 \eta_s$ via FSIs, the matrix c^2 arising from two D -type couplings in the $I = 1/2$ sector has the form

$$c^2 \propto \kappa^2 \begin{pmatrix} \frac{3}{2} & \frac{\sqrt{3}}{2} & \frac{\sqrt{3}}{\sqrt{2}} \\ \frac{\sqrt{3}}{2} & \frac{1}{2} & \frac{1}{\sqrt{2}} \\ \frac{\sqrt{3}}{\sqrt{2}} & \frac{1}{\sqrt{2}} & 1 \end{pmatrix} \quad (3.6)$$

in the basis of $(\bar{K}\pi)_{1/2}$, $\bar{K}^0 \eta_q$, $\bar{K}^0 \eta_s$. Since $\sum |c_{ij}|^2 = 3\kappa^2$, it follows that the normalized matrix c^2 reads

$$c^2 \equiv \hat{c} = \begin{pmatrix} \frac{1}{2} & \frac{1}{2\sqrt{3}} & \frac{1}{\sqrt{6}} \\ \frac{1}{2\sqrt{3}} & \frac{1}{6} & \frac{1}{3\sqrt{2}} \\ \frac{1}{\sqrt{6}} & \frac{1}{3\sqrt{2}} & \frac{1}{3} \end{pmatrix}. \quad (3.7)$$

Then it is easily seen that

$$A(D^0 \rightarrow \bar{K}^0 \eta_s) = \mathcal{E} = e + (e^{2i\delta_r} - 1) \left[\frac{1}{\sqrt{6}} A(D^0 \rightarrow (\bar{K}\pi)_{1/2}) + \frac{1}{3\sqrt{2}} A(D^0 \rightarrow \bar{K}^0 \eta_q) + \frac{1}{3} A(D^0 \rightarrow \bar{K}^0 \eta_s) \right], \quad (3.8)$$

and hence

$$\mathcal{E} = e + (e^{2i\delta_r} - 1) \left(e + \frac{t}{3} \right), \quad (3.9)$$

where we have used t, c, e, a to denote the corresponding reduced amplitudes $\mathcal{T}, \mathcal{C}, \mathcal{E}, \mathcal{A}$ before resonant FSIs.⁶ Likewise, it is straightforward to show that $\mathcal{T} = t$ and $\mathcal{C} = c$.

⁶ The quark-graph amplitudes listed in Table 1 are those after the inclusion of FSIs

Therefore, resonance-induced FSIs amount to modifying the W -exchange amplitude and leaving the other quark-diagram amplitudes \mathcal{T} and \mathcal{C} intact. We thus see that even if the short-distance W -exchange vanishes (i.e. $e = 0$), as commonly asserted, a long-distance W -exchange contribution still can be induced from the tree amplitude \mathcal{T} via FSIs in resonance formation.⁷

Likewise, from Cabibbo-allowed decays $D_s^+ \rightarrow \bar{K}^0 K^+$, $\pi^+ \eta_q$ and $\pi^+ \eta_s$ one can show that the W -annihilation amplitude after resonant FSIs reads

$$\mathcal{A} = a + (e^{2i\delta_r} - 1) \left(a + \frac{\mathcal{C}}{3} \right). \quad (3.10)$$

Note that, contrary to the W -exchange case, the long-distance W -annihilation amplitude is induced from the color-suppressed internal W -emission.

As for the W -exchange graph in $D \rightarrow \bar{K}^* \pi$ and $\bar{K} \rho$ decays, we consider a 0^- resonance P' which couples to VP and PV states with the F -type coupling, $\kappa' \text{Tr}(P'[V, P])$. Proceeding as before, the 6×6 normalized coupling matrix reads

$$c^2 = \frac{1}{2} \begin{pmatrix} \hat{c} & -\hat{c} \\ -\hat{c} & \hat{c} \end{pmatrix} \quad (3.11)$$

in the basis of $(\bar{K}^* \pi)_{1/2}$, $\bar{K}^{*0} \eta_q$, $\phi \bar{K}^0$, $(\bar{K} \rho)_{1/2}$, $\bar{K}^0 \omega$ and $\eta_s \bar{K}^{*0}$, where \hat{c} is the matrix given by (3.7) and

$$\begin{aligned} A(D^0 \rightarrow (\bar{K}^* \pi)_{3/2}) &= \frac{1}{\sqrt{3}}(\mathcal{T}_V + \mathcal{E}_P), \\ A(D^0 \rightarrow (\bar{K}^* \pi)_{1/2}) &= \frac{1}{\sqrt{6}}(2\mathcal{T}_V - \mathcal{C}_P + 3\mathcal{E}_P), \\ A(D^0 \rightarrow (\bar{K} \rho)_{3/2}) &= \frac{1}{\sqrt{3}}(\mathcal{T}_P + \mathcal{E}_V), \\ A(D^0 \rightarrow (\bar{K} \rho)_{1/2}) &= \frac{1}{\sqrt{6}}(2\mathcal{T}_P - \mathcal{C}_V + 3\mathcal{E}_V). \end{aligned} \quad (3.12)$$

It is straightforward to show that $\mathcal{T}_{P,V}$ and $\mathcal{C}_{P,V}$ are not affected by resonant FSIs and

$$\begin{aligned} \mathcal{E}_P &= e_P + \frac{1}{2}(e^{2i\delta_r} - 1) \left[e_P - e_V + \frac{1}{3}(\mathcal{T}_V - \mathcal{T}_P) \right], \\ \mathcal{E}_V &= e_V + \frac{1}{2}(e^{2i\delta_r} - 1) \left[e_V - e_P + \frac{1}{3}(\mathcal{T}_P - \mathcal{T}_V) \right], \end{aligned} \quad (3.13)$$

⁷ An expression similar to (3.9),

$$\mathcal{E} = e + (\cos \delta e^{i\delta} - 1) \left(e + \frac{\mathcal{T}}{3} \right),$$

was first obtained by Zenczykowski [34] by applying the strong reaction matrix K_0 together with the unitarity constraint of the S matrix to study the effects of resonance-induced FSIs. However, since $(e^{2i\delta_r} - 1) = 2(\cos \delta_r e^{i\delta_r} - 1)$, it is clear that the contribution of resonant FSIs to the W -exchange amplitude as given above is too small by a factor of 2. This has been corrected in [23]

or

$$\begin{aligned} \mathcal{E}_P + \mathcal{E}_V &= e_P + e_V, \\ \mathcal{E}_P - \mathcal{E}_V &= e_P - e_V \\ &+ (e^{2i\delta_r} - 1) \left(e_P - e_V - \frac{1}{3}(\mathcal{T}_P - \mathcal{T}_V) \right). \end{aligned} \quad (3.14)$$

Note that the terms in square brackets in (3.13) have opposite signs for \mathcal{E}_P and \mathcal{E}_V owing to the charge conjugation of the strong coupling.⁸ We will come back to this point later.

As for the W -annihilation amplitudes \mathcal{A}_P and \mathcal{A}_V , a direct analysis of resonant FSIs in Cabibbo-allowed decays $D_s^+ \rightarrow \rho\pi, \rho^+\eta(\eta')$, $\omega\pi^+, \phi\pi^+, \bar{K}^{*0} K$ shows that the reduced amplitudes $\mathcal{T}_{P,V}$ and $\mathcal{A}_P + \mathcal{A}_V$ are not affected by FSIs in resonance formation

$$\mathcal{T}_P = t_P, \quad \mathcal{T}_V = t_V, \quad \mathcal{A}_P + \mathcal{A}_V = a_P + a_V. \quad (3.15)$$

The relevant normalized coupling matrix in the basis of $(\rho\pi)_1, \bar{K}^{*0} K^+$ and $K^{*+} \bar{K}^0$ is given by

$$c^2 = \begin{pmatrix} \frac{2}{3} & \frac{1}{3} & -\frac{1}{3} \\ \frac{1}{3} & \frac{1}{6} & -\frac{1}{6} \\ -\frac{1}{3} & -\frac{1}{6} & \frac{1}{6} \end{pmatrix}, \quad (3.16)$$

where

$$\begin{aligned} A(D_s^+ \rightarrow (\rho\pi)_1) &= \frac{1}{\sqrt{2}}[A(D_s^+ \rightarrow \rho^0\pi^+) - A(D_s^+ \rightarrow \rho^+\pi^0)] = \mathcal{A}_P - \mathcal{A}_V, \\ A(D_s^+ \rightarrow (\rho\pi)_2) &= \frac{1}{\sqrt{2}}[A(D_s^+ \rightarrow \rho^0\pi^+) + A(D_s^+ \rightarrow \rho^+\pi^0)] = 0. \end{aligned} \quad (3.17)$$

It follows that

$$\begin{aligned} \mathcal{A}_P + \mathcal{A}_V &= a_P + a_V, \\ \mathcal{A}_P - \mathcal{A}_V &= a_P - a_V \\ &+ (e^{2i\delta_r} - 1) \left(a_P - a_V + \frac{1}{3}(\mathcal{C}_P - \mathcal{C}_V) \right), \end{aligned} \quad (3.18)$$

and $\mathcal{C}_{P,V}$ are not affected. This result was first obtained by Zenczykowski [34]. Note the similarity between the expressions of (3.18) and (3.14).

The fact that the amplitudes \mathcal{T} and \mathcal{C} are not affected by resonance-induced FSIs has an important implication. At first sight, it appears that the \mathcal{T} amplitude can be converted into the \mathcal{E} amplitude in D^0 decay via a quark-pair annihilation in the final state (see Fig. 1) but not in D^+ decay. Consequently, the value of \mathcal{T} in D^0 decay is no longer the same as that in D^+ decay after long-distance interactions enter since part of \mathcal{T} turns into \mathcal{E} for D^0 decay.

⁸ The expression of (3.13) or (3.14) differs from the results obtained in [34, 22] for \mathcal{E}_P and \mathcal{E}_V

However, we have shown that it is not the case. In fact, the total rate of $D^0 \rightarrow (\bar{K}\pi)_{1/2}, \bar{K}^0\eta_q, \bar{K}^0\eta_s$ remains the same after resonant FSIs, namely (assuming $e = 0$ for simplicity and ignoring the phase-space differences),

$$\begin{aligned} & \frac{1}{6}|2\mathcal{T} - \mathcal{C} + 3\mathcal{E}|^2 + \frac{1}{2}|\mathcal{C} + \mathcal{E}|^2 + |\mathcal{E}|^2 \\ &= \frac{1}{6}|2\mathcal{T} - \mathcal{C}|^2 + \frac{1}{2}|\mathcal{C}|^2. \end{aligned} \quad (3.19)$$

The above relation holds for arbitrary \mathcal{T} and \mathcal{C} amplitudes as long as \mathcal{E} satisfies (3.9) with $e = 0$. Therefore, although the long-distance \mathcal{E} amplitude is induced from the quark diagram \mathcal{T} via resonant FSIs, the latter is not affected by long-distance interactions. This feature explains why one can assign *common* \mathcal{T} and \mathcal{C} amplitudes for D^0 , D^+ and D_s^+ decays and why the weak decay processes can be classified in a sensible way in terms of quark-graph amplitudes.

3.2 Phenomenological implications

3.2.1 Resonance-induced weak annihilations

Equations (3.9), (3.10), (3.14) and (3.18) are the main results for weak annihilation amplitudes induced from FSIs in resonance formation. We see that even in the absence of the short-distance weak annihilation, a long-distance weak annihilation can be induced via resonant FSIs. For parity-violating $D \rightarrow PP$ decays, there is a $J^P = 0^+$ resonance $K_0^*(1950)$ in the $s\bar{d}$ quark content with mass $1945 \pm 10 \pm 20$ MeV and width $201 \pm 34 \pm 79$ MeV [15]. Assuming $e = 0$ in (3.9), we obtain

$$\mathcal{E} = 1.43 \times 10^{-6} \exp(i143^\circ) \text{ GeV}, \quad (3.20)$$

which is close to the ‘‘experimental’’ value $\mathcal{E} = (1.60 \pm 0.13) \times 10^{-6} \exp(i114^\circ) \text{ GeV}$ [cf. (2.9)]. Presumably, a non-vanishing short-distance e will bring the phase of \mathcal{E} in agreement with experiment. Resonance-induced coupled-channel effects are governed by the width and mass of nearby resonances, which are unfortunately not well determined. For example, a reanalysis in a K -matrix formalism [40] quotes $m_R = 1820 \pm 40$ MeV and $\Gamma = 250 \pm 100$ MeV for the same resonance. This leads to $\mathcal{E} = 1.67 \times 10^{-6} \exp(-i158^\circ) \text{ GeV}$. Therefore, we conclude that one needs a 0^+ resonance heavier than the charmed meson. Contributions from the more distance resonance at 1430 MeV are smaller (see also [38, 41]).

Since a nearby 0^+ resonance a_0 in the charm mass region has not been observed, we will not make an estimate of the resonance-induced W -annihilation amplitude in Cabibbo-allowed $D \rightarrow PP$ decay. In the factorization approach, it is expected that $\mathcal{E}/\mathcal{A} \sim a_2/a_1$ and hence $|\mathcal{A}| > |\mathcal{E}|$. Nevertheless, it is clear from (3.10) that the long-distance W -annihilation is slightly smaller than the W -exchange one because the former is induced from the color-suppressed amplitude \mathcal{C} and this is consistent with (3.9).

To estimate the resonance-induced W -annihilation amplitude $\mathcal{A}_P - \mathcal{A}_V$, we employ $\pi(1800)$ as the appropriate 0^- resonance with $m_R = 1801 \pm 13$ MeV and $\Gamma = 210 \pm 15$ MeV [15]. Assuming $a_P - a_V = 0$, we find from (3.18) that

$$|\mathcal{A}_P - \mathcal{A}_V| = 2.4 \times 10^{-7}, \quad (3.21)$$

which is in agreement with the experimental value given by (2.18). Note that if we set $a_P = a_V = 0$, this will lead to $\mathcal{A}_V = -\mathcal{A}_P$ which will imply a vanishing $D_s^+ \rightarrow \pi^+\omega$, in contradiction to the experimental observation.

3.2.2 Hadronic D decays to η or η'

Weak annihilation effects are crucial for some two-body decays involving one single isospin component, e.g. the final state containing an η and η' . This has been discussed in detail in [22, 23, 41, 42]. To see this, we consider the Cabibbo-allowed decays $D^0 \rightarrow \bar{K}^0(\eta, \eta')$ and Cabibbo-suppressed modes $D^+ \rightarrow \pi^+(\eta, \eta')$. In realistic calculations we use the η - η' mixing angle $\theta = -15.4^\circ$, but it suffices for our purposes to use $\theta = -19.5^\circ$ to discuss the essence of physics. The quark-graph amplitudes then read

$$\begin{aligned} A(D^0 \rightarrow \bar{K}^0 \eta) &= \mathcal{C}/\sqrt{3}, \\ A(D^0 \rightarrow \bar{K}^0 \eta') &= (\mathcal{C} + 3\mathcal{E})/\sqrt{6}, \\ A(D^+ \rightarrow \pi^+ \eta) &= \frac{V_{cd}}{V_{cs}} \frac{1}{\sqrt{3}} (\mathcal{T} + 2\mathcal{C} + 2\mathcal{A}), \\ A(D^+ \rightarrow \pi^+ \eta') &= \frac{V_{cd}}{V_{cs}} \frac{1}{\sqrt{6}} (\mathcal{T} - \mathcal{C} + 2\mathcal{A}). \end{aligned} \quad (3.22)$$

Since \mathcal{E} is comparable to the color-suppressed \mathcal{C} in magnitude, the decay $D^0 \rightarrow \bar{K}^0 \eta'$ is largely enhanced by W -exchange. We see from Table 6 that its branching ratio is enhanced by resonance-induced FSIs by almost one order of magnitude, whereas $D^0 \rightarrow \bar{K}^0 \eta$ remains essentially unaffected. Therefore, we conclude that it is the W -exchange effect that accounts for the bulk of $\mathcal{B}(D^0 \rightarrow \bar{K}^0 \eta')$ and explains why $\bar{K}^0 \eta' > \bar{K}^0 \eta$.

As for $D^+ \rightarrow \pi^+(\eta, \eta')$ decays, it is clear from (2.9) that the interference is constructive between $2\mathcal{A}$ and $\mathcal{T} + 2\mathcal{C}$ and destructive between $2\mathcal{A}$ and $\mathcal{T} - \mathcal{C}$. Hence, the presence of W -annihilation is crucial for understanding the data of $D^+ \rightarrow \pi^+ \eta$ (see Table 6).

3.3 Difficulties with the weak annihilation amplitudes $\mathcal{E}_{P,V}$ and $\mathcal{A}_{P,V}$

For the W -exchange amplitude in $D \rightarrow VP$ decays, at first sight it appears that its sign flip from \mathcal{E}_P to \mathcal{E}_V can be naturally explained since the 0^- resonance is expected to have equal and opposite couplings to $K^{*-}\pi^+$ and $K^-\rho^+$, as shown in (3.13). It is obvious from (3.14) that $\mathcal{E}_P = -\mathcal{E}_V$ in the absence of short-distance W -exchange contributions. However, a further study shows some problems.

Table 6. Branching ratios (in percent) of the charmed meson decays to an η or η'

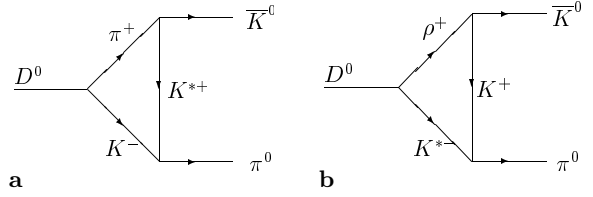
Decay	Without weak annihilation	With weak annihilation	Expt. [15]
$D^0 \rightarrow \bar{K}^0 \eta$	0.64	0.66	0.70 ± 0.10
$D^0 \rightarrow \bar{K}^0 \eta'$	0.31	1.76	1.71 ± 0.26
$D^+ \rightarrow \pi^+ \eta$	0.09	0.37	0.30 ± 0.06
$D^+ \rightarrow \pi^+ \eta'$	0.27	0.39	0.50 ± 0.10

First, a possible candidate of the 0^- resonance near m_D is the $K(1830)$ with mass ~ 1830 MeV and width ~ 250 MeV [15], but only the $K\phi$ decay mode has been reported. Second, due to the F -type coupling of the resonance with VP states, the resonance contribution from the leading tree amplitude \mathcal{T} is proportional to the difference $\mathcal{T}_P - \mathcal{T}_V$, which is small. Assuming $e_P = e_V = 0$ for the moment, we obtain from (2.10), (2.16) and (3.13) that

$$\mathcal{E}_P = -\mathcal{E}_V = 1.6 \times 10^{-7} \exp(i17^\circ) \quad (3.23)$$

from the resonance $K(1830)$. Evidently, \mathcal{E}_P and \mathcal{E}_V are *not* governed by resonant FSIs, contrary to the original conjecture advocated in [10]. In order to explain the sign flip of the W -exchange amplitude, it appears that the (short-distance) W -exchange amplitudes e_P and e_V have to be sizable in magnitude and opposite in signs or the 0^- resonance couples strongly to one of the $K^{*-}\pi^+$ and $K^-\rho^+$ states, or the long-distance t -channel effect analogous to Fig. 2b, which has been ignored thus far, gives the dominant contributions to \mathcal{E}_P and \mathcal{E}_V with opposite signs. In any of these cases, it is not clear what the underlying physics is. Therefore, the sign flip of the W -exchange amplitude in Cabibbo-allowed VP decays remains unexplained.

We also face some difficulties for understanding the W -annihilation amplitudes \mathcal{A}_P and \mathcal{A}_V in $D \rightarrow VP$ decays. This is because naively one will expect that $D_s^+ \rightarrow \pi^+\omega$ is suppressed relative to $D_s^+ \rightarrow \pi^+\rho^0$. The argument goes as follows. The direct W -annihilation contributions via $c\bar{s} \rightarrow W \rightarrow u\bar{d}$ are not allowed in $D_s^+ \rightarrow \pi^+\omega, \rho^+\eta, \rho^+\eta'$ decays since the $(u\bar{d})$ has zero total angular momentum and hence it has the quantum number of π^+ . Therefore, $G(u\bar{d}) = -$ and the final states should have odd G -parity. Since G -parity is even for $\omega\pi^+$ and odd for $\pi^+\rho^0$, it is clear that the former does not receive a direct W -exchange contribution. Can one induce $D_s^+ \rightarrow \pi^+\omega$ from resonant FSIs? The answer is no, because the $J = 0, I = 1$ meson resonance made from a quark-antiquark pair $u\bar{d}$ has odd G -parity. As stressed in [43], the even- G state $\pi^+\omega$ (also $\rho\eta$ and $\rho\eta'$) does not couple to any single meson resonances, nor to the state produced by the W -annihilation diagram with no gluons emitted by the initial state before annihilation. This is indeed consistent with (3.18) which states that, contrary to $\mathcal{A}_P - \mathcal{A}_V$, $\mathcal{A}_P + \mathcal{A}_V$ does not receive any $q\bar{q}'$ resonance contributions. Therefore, it will be expected that $D_s^+ \rightarrow \pi^+\omega$ is prohibited (or $\mathcal{A}_V \approx -\mathcal{A}_P$), whereas $D_s^+ \rightarrow \pi^+\rho^0$ receives both factorizable and resonance-induced W -annihilation contributions. Ex-

**Fig. 3a,b.** Manifestation of Fig. 1b as the long-distance t -channel contributions to the color-suppressed internal W -emission amplitude in $D^0 \rightarrow \bar{K}^0 \pi^0$

perimentally, it is the other way around: $\mathcal{B}(D_s^+ \rightarrow \pi^+\omega) = (2.8 \pm 1.1) \times 10^{-3}$ [44] and $\mathcal{B}(D_s^+ \rightarrow \pi^+\rho^0) \sim 6 \times 10^{-4}$ [19]. Hence, it is important to understand the origin of the W -annihilation contribution. As noted in passing, (2.17) and (2.18) suggest that the phase difference between \mathcal{A}_P and \mathcal{A}_V is less than 90° and that the magnitude of \mathcal{A}_P or \mathcal{A}_V is smaller than \mathcal{E}_P and \mathcal{E}_V , contrary to the PP case. The suppression of W -annihilation is expected because of the G -parity constraint. Since W -annihilation occurs only in the D_s^+ system for Cabibbo-allowed decays, its suppression may help to explain why $\tau(D_s^+) > \tau(D^0)$ at the two-body or quasi-two-body decay level.

4 Color-suppressed internal W -emission amplitude

The relative phase between \mathcal{T} and \mathcal{C} indicates some final-state interactions responsible for this. Figure 1b shows that final-state rescattering via quark exchange has the same topology as the color-suppressed internal W -emission amplitude. At the hadron level, Fig. 1b is manifested as FSIs with one-particle exchange in the t -channel [45, 32]; see Fig. 3. Note that although Fig. 3 is very similar to Fig. 2b, the exchanged particles here are K^* and K rather than ρ and π . Another approach is based on the Regge pole model [32]. Admittedly, the estimate of Fig. 3 is subject to some theoretical uncertainties as discussed before, e.g. the off-shell form factor appearing in the chiral-loop calculation is unknown. Nevertheless, we still can learn something useful. For example, Li and Zou [45] have calculated rescattering FSIs for $D^+ \rightarrow \bar{K}^{*0} \pi^+$ and $D^+ \rightarrow \bar{K}^0 \rho^+$ via single pion exchange. The absorptive part of the chiral-loop diagram in analogy to Fig. 3 gives the imaginary contribution to the FSI amplitude. It was found that the imaginary part is negative for \mathcal{C}_P and \mathcal{C}_V (see Table II of [45]). This lends support to the solution set (i) in (2.16). We will leave a detailed study of this inelastic FSI effect to a separate publication.

It is often argued that the relative phase between \mathcal{T} and \mathcal{C} can be understood in the factorization approach as arising from the rescattering through modifications of the phases of isospin amplitudes [14, 35, 10]. First, one identifies the isospin amplitudes with the factorizable amplitudes before the final-state phases are turned on in (2.8). For example, $A(D^+ \rightarrow \bar{K}^0 \pi^+) = 3^{1/2} A_{3/2} = T_f + C_f$.

This leads to the isospin amplitudes

$$\begin{aligned} A_{1/2} &= \frac{1}{\sqrt{6}}(2T_f - C_f + 3E_f), \\ A_{3/2} &= \frac{1}{\sqrt{3}}(T_f + C_f), \end{aligned} \quad (4.1)$$

where T_f, C_f, E_f are the factorizable tree, color-suppressed, and W -exchange amplitudes, respectively. Second, after introducing isospin phases to (2.8), it is straightforward to show that

$$\begin{aligned} \mathcal{T} + \mathcal{E} &= (T_f + E_f)e^{i\delta_{1/2}} - \frac{1}{3}(T_f + C_f)(e^{i\delta_{1/2}} - e^{i\delta_{3/2}}), \\ \mathcal{C} - \mathcal{E} &= (C_f - E_f)e^{i\delta_{1/2}} \\ &\quad - \frac{2}{3}(T_f + C_f)(e^{i\delta_{1/2}} - e^{i\delta_{3/2}}). \end{aligned} \quad (4.2)$$

Therefore, the different phases of \mathcal{C} and \mathcal{T} are a consequence of rescattering. This has an important implication for the class-II mode $D^0 \rightarrow \bar{K}^0 \pi^0$. Even if the factorizable C_f and E_f amplitudes are small, the weak decay $D^0 \rightarrow K^- \pi^+$ followed by the inelastic rescattering $K^- \pi^+ \rightarrow \bar{K}^0 \pi^0$ can increase $\mathcal{B}(D^0 \rightarrow \bar{K}^0 \pi^0)$ dramatically and lower $\mathcal{B}(D^0 \rightarrow K^- \pi^+)$ slightly.

Of course, the above picture for rescattering is too simplified and it does not offer a genuine explanation of the phases of the quark-graph amplitudes \mathcal{C} and \mathcal{T} . First, the decays $\bar{K}^0 \eta$ and $\bar{K}^0 \eta'$ have only one isospin component and the above analysis does not give a clue as to why they are not color suppressed. Second, the isospin phase difference in $D \rightarrow \bar{K} \rho$ decays is near zero and yet a relative phase of order 150° between \mathcal{C} and \mathcal{T} is found in the diagrammatic approach [see (2.16)]. Third, the above isospin analysis has no power of prediction as the phase difference is unknown from the outset; even if elastic $\bar{K} \pi$ scattering is measured at energies $s^{1/2} = m_D$, the isospin phases appearing in (2.8) and (4.2) cannot be identified with the measured strong phases.⁹

5 Comparison with B decays

It is instructive to compare the present study with the B decays. To proceed, we quote some of the results for $\bar{B} \rightarrow D\pi, D^* \pi$ decays [29]:

$$\begin{aligned} \bar{B} \rightarrow D\pi : \quad \frac{A_{1/2}}{A_{3/2}} &= (1.00 \pm 0.14)e^{i29^\circ}, \\ \frac{a_2}{a_1} &= (0.40 \sim 0.65)e^{i59^\circ}, \end{aligned}$$

⁹ If there are only a few channels open as in the case of two-body non-leptonic decays of kaons and hyperons, the isospin phases there (or decay amplitude phases) are related to strong-interaction eigenphases. However, when there are many channels open and some channels coupled, as in D and especially B decays, the decay phase is no longer the same as the eigenphase in the S -matrix

$$\begin{aligned} \bar{B} \rightarrow D^* \pi : \quad \frac{A_{1/2}}{A_{3/2}} &= (1.05 \pm 0.10)e^{i29^\circ}, \\ \frac{a_2}{a_1} &= (0.30 \sim 0.55)e^{i63^\circ}. \end{aligned} \quad (5.1)$$

The relative phase between a_1 and a_2 is of order 60° . The QCD factorization approach [5] implies that $\delta_{1/2} - \delta_{3/2} = \mathcal{O}(\Lambda_{\text{QCD}}/m_Q)$ and $A_{1/2}/(2^{1/2}A_{3/2}) = 1 + \mathcal{O}(\Lambda_{\text{QCD}}/m_Q)$. We see that, except for $D \rightarrow \bar{K} \rho$, the isospin phase difference indeed decreases from charm (of order $90^\circ \sim 100^\circ$) to the bottom system and the ratio of isospin amplitudes in D decays shows a sizable departure from the heavy quark limit. The relative phase of a_1 and a_2 is crucial for understanding the destructive interference in the class-III mode $D^+ \rightarrow \bar{K}^0 \pi^+$ and the constructive interference in $B^- \rightarrow D^0 \pi^-$.

Since the color-suppressed mode $B \rightarrow J/\psi K$ does not receive any weak annihilation contribution and the penguin contribution to this decay is very tiny, the parameter a_2 can be directly determined from experiment with the result $|a_2(B \rightarrow J/\psi K)| = 0.26 \pm 0.02$ [46]. It is evident that even in B decays, a_2 varies from channel to channel.

In obtaining (5.1) we have neglected the W -exchange amplitudes in $\bar{B} \rightarrow D^{(*)} \pi$ decays. It is generally argued that weak annihilation is negligible as helicity suppression should be more effective due to the large energy release in B decays. Owing to the absence of nearby resonances in the B mass region, the weak annihilation amplitude will not be dominated by resonance-induced FSIs, contrary to the charm case. Hence, the formalism developed in Sect. 3 for D decays is not applicable to B mesons.

Recently, there have been recognized some growing hints that penguin-induced weak annihilation is important. For example, the theory predictions of the charmless B decays to $\bar{K}^* \pi, \bar{K} \rho$ and $\bar{K}^* \eta$ based on QCD factorization are too small by one order of magnitude in the decay rates [47]. This implies that the weak annihilation (denoted P_e or P_a in the literature) may play an essential role. Indeed, a recent calculation based on the hard scattering pQCD approach indicates that the $\bar{K}^* \pi$ modes are dominated by penguin-induced annihilation diagrams [48]. This is understandable because the usual helicity suppression argument works only for the weak annihilation diagram produced from $(V-A)(V-A)$ operators. However, weak annihilations induced by the $(S-P)(S+P)$ penguin operators are no longer subject to helicity suppression and hence can be sizable.

It is anticipated that the soft FSI contributions to the color-suppressed topology \mathcal{C} are dominated by inelastic rescattering [49]. As for the phase of the ratio of a_2/a_1 , the rescattering contribution via quark exchange, $D^+ \pi^- \rightarrow D^0 \pi^0$, to the topology \mathcal{C} in $\bar{B}^0 \rightarrow D^0 \pi^0$ has been estimated in [50] using ρ trajectory Regge exchange. It was found that the additional contribution to $D^0 \pi^0$ from rescattering is mainly imaginary: $a_2(D\pi)/a_2(D\pi)_{\text{without FSIs}} = 1 + 0.61 \exp(73^\circ)$. This analysis suggests that the rescattering amplitude can bring about a large phase to $a_2(D\pi)$ as expected.

6 Conclusions

We have presented a study of hadronic charm decays within the framework of the diagrammatic approach. We draw some conclusions from the analysis.

(1) Based on SU(3) symmetry, many of the topological quark-graph amplitudes for Cabibbo-allowed D decays can be extracted from the data. The ratio of a_2/a_1 has the magnitude of order 0.60, 0.40 and 0.83 for $D \rightarrow \bar{K}\pi, \bar{K}^*\pi, \bar{K}\rho$ decays, respectively, with a phase of order 150° . This implies that non-factorizable corrections to $\bar{K}\rho$ are far more important than $\bar{K}^*\pi$.

(2) Except for the W -annihilation topology in VP decays, the weak annihilation (W -exchange or W -annihilation) amplitude has a sizable magnitude comparable to the color-suppressed internal W -emission with a large phase relative to the tree amplitude. It receives long-distance contributions from nearby resonance via inelastic final-state interactions from the leading tree or color-suppressed amplitude. The effects of resonance-induced FSIs can be described in a model independent manner and are governed by the mass and decay width of the nearby resonances.

(3) Weak annihilation topologies in $D \rightarrow PP$ decays are dominated by nearby scalar resonances via final-state rescattering. In contrast, W -exchange in VP systems receives little contributions from resonant final-state interactions.

(4) The experimental data indicate that the three decay amplitudes of $D \rightarrow \bar{K}\rho$ are essentially in phase with one another. This requires that either the W -exchange amplitudes in $\bar{K}\rho$ and $\bar{K}^*\pi$ have opposite signs or the relative phase between the tree and color-suppressed amplitudes flips the sign. While the latter possibility is probably ruled out by the measurement of $D^0 \rightarrow \bar{K}^{*0}\eta$ and by the model calculation of the phase of the color-suppressed amplitude, the first possibility is hampered by the observation that dominance of nearby resonances is not operative for the W -exchange contribution in Cabibbo-allowed $D \rightarrow VP$ decays. Therefore, why the sign of the W -exchange amplitude flips in $D \rightarrow \bar{K}^*\pi$ and $\bar{K}\rho$ decays remains unexplained.

(5) Owing to the G -parity constraint, the W -annihilation amplitude \mathcal{A}_P or \mathcal{A}_V in $D \rightarrow VP$ decays is suppressed relative to W -exchange, contrary to the $D \rightarrow PP$ case where W -exchange and W -annihilation are comparable. Since W -annihilation occurs only in the D_s^+ system for Cabibbo-allowed decays, this may help to explain the longer lifetime of D_s^+ than D^0 .

(6) Weak annihilation contributions are crucial for understanding the data of $D^0 \rightarrow \bar{K}^0\eta'$ and $D^+ \rightarrow \pi^+\eta$.

(7) The relative phase between the tree and color-suppressed amplitudes arises from the final-state rescattering via quark exchange. This can be evaluated by considering the t -channel chiral-loop effect or by applying the Regge pole method. Much more work along this line is needed.

(8) Some Cabibbo-suppressed modes exhibit huge SU(3) flavor symmetry breaking effects. This can be accounted

for by the accumulation of several modest SU(3) violations in individual quark-graph amplitudes.

Acknowledgements. We wish to thank C.N. Yang Institute for Theoretical Physics at SUNY Stony Brook for its hospitality. This work was supported in part by the National Science Council of R.O.C. under Grant No. NSC90-2112-M-001-047.

References

1. M. Fukugita, T. Inami, N. Sakai, S. Yazaki, Phys. Lett. B **72**, 237 (1977); D. Tadić, J. Trampetić, ibid. B **114**, 179 (1982); M. Bauer, B. Stech, ibid. B **152**, 380 (1985)
2. A.J. Buras, J.-M. Gérard, R. Rückl, Nucl. Phys. B **268**, 16 (1986)
3. B. Blok, M. Shifman, Sov. J. Nucl. Phys. **45**, 35, 301, 522 (1987)
4. I. Halperin, Phys. Lett. B **349**, 548 (1995)
5. M. Beneke, G. Buchalla, M. Neubert, C.T. Sachrajda, Phys. Rev. Lett. **83**, 1914 (1999); Nucl. Phys. B **591**, 313 (2000); ibid. B **606**, 245 (2001)
6. J.F. Donoghue, Phys. Rev. D **33**, 1516 (1986)
7. L.L. Chau, H.Y. Cheng, Phys. Rev. D **36**, 137 (1987); Phys. Lett. B **222**, 285 (1989)
8. L.L. Chau, Phys. Rep. **95**, 1 (1983)
9. L.L. Chau, H.Y. Cheng, Phys. Rev. Lett. **56**, 1655 (1986)
10. J.L. Rosner, Phys. Rev. D **60**, 114026 (1999)
11. L.L. Chau, H.Y. Cheng, Phys. Rev. D **39**, 2788 (1989); L.L. Chau, H.Y. Cheng, T. Huang, Z. Phys. C **53**, 413 (1992)
12. X.Y. Li, S.F. Tuan, DESY Report No. 83-078 (unpublished); X.Y. Li, X.Q. Li, P. Wang, Nuovo Cimento A **100**, 693 (1988)
13. A.S. Dighe, M. Gronau, J.L. Rosner, Phys. Rev. Lett. **79**, 4333 (1997)
14. H.J. Lipkin, Phys. Rev. Lett. **44**, 710 (1980)
15. Particle Data Group, D.E. Groom et al., Eur. Phys. J. C **15**, 1 (2000)
16. L.L. Chau, H.Y. Cheng, W.K. Sze, H. Yao, B. Tseng, Phys. Rev. D **43**, 2176 (1991)
17. T. Feldmann, P. Kroll, Eur. Phys. J. C **5**, 327 (1998); T. Feldmann, P. Kroll, B. Stech, Phys. Rev. D **58**, 114006 (1998); Phys. Lett. B **449**, 339 (1999); T. Feldmann, P. Kroll, hep-ph/0201044
18. F.E. Close, H.J. Lipkin, Phys. Lett. B **405**, 157 (1997)
19. Fermilab E791 Collaboration, E.M. Aitala et al., Phys. Rev. Lett. **86**, 765 (2001)
20. F. Buccella, M. Lusignoli, A. Pugliese, Phys. Lett. B **379**, 249 (1996); F. Buccella, M. Lusignoli, G. Miele, A. Pugliese, P. Santorelli, Phys. Rev. D **51**, 3478 (1995)
21. P. Ball, J.-M. Frère, M. Tytgat, Phys. Lett. B **365**, 367 (1996)
22. H.Y. Cheng, B. Tseng, Phys. Rev. D **59**, 014034 (1999)
23. H.Y. Cheng, B. Tseng, Chin. J. Phys. **39**, 28 (2001) [hep-ph/0006081]
24. M. Wirbel, B. Stech, M. Bauer, Z. Phys. C **29**, 637 (1985); M. Bauer, B. Stech, M. Wirbel, ibid. C **34**, 103 (1987)
25. D. Melikhov, B. Stech, Phys. Rev. D **62**, 014006 (2001)
26. CLEO Collaboration, A. Bean et al., Phys. Lett. B **317**, 647 (1993)
27. A. Khodjamirian, R. Rückl, S. Weinzierl, C.W. Winhart, O. Yakovlev, Phys. Rev. D **62**, 114002 (2000)

28. A. Abada et al., Nucl. Phys. B **619**, 565 (2001)
29. H.Y. Cheng, Phys. Rev. D **65**, 094012 (2002)
30. G. Buchalla, A.J. Buras, M.E. Lautenbacher, Rev. Mod. Phys. **68**, 1125 (1996)
31. L.L. Chau, H.Y. Cheng, Phys. Lett. B **333**, 514 (1994)
32. Y.S. Dai, D.S. Du, X.Q. Li, Z.T. Wei, B.S. Zou, Phys. Rev. D **60**, 014014 (1999)
33. J.O. Eeg, S. Fajfer, J. Zupan, Phys. Rev. D **64**, 034010 (2001)
34. P. Żenczykowski, Acta Phys. Polon. B **28**, 1605 (1997) [hep-ph/9601265]
35. M. Neubert, Phys. Lett. B **424**, 152 (1998)
36. El hassan El aaoud, A.N. Kamal, Int. J. Mod. Phys. A **15**, 4163 (2000)
37. M. Ablikim, D.S. Du, M.Z. Yang, Phys. Lett. B **536**, 34 (2002)
38. M. Gronau, Phys. Rev. Lett. **83**, 4005 (1999)
39. S. Weinberg, The quantum theory of fields, Volume I (Cambridge, 1995), Section 3.8
40. A.V. Anisovich, A.V. Sarantsev, Phys. Lett. B **413**, 137 (1997)
41. S. Fajfer, J. Zupan, Int. J. Mod. Phys. A **14**, 4161 (1999)
42. T.N. Pham, Phys. Rev. D **46**, 2080 (1992); A.N. Kamal, Q.P. Xu, A. Czarnecki, ibid. D **48**, 5215 (1993); P. Bedaque, A. Das, V.S. Mathur, ibid. D **49**, 269 (1994); B. Bajc, S. Fajfer, R.J. Oakes, S. Prelovsek, ibid. D **56**, 7207 (1997); P. Colangelo, F. De Fazio, Phys. Lett. B **520**, 78 (2001)
43. H.J. Lipkin, Phys. Lett. B **283**, 412 (1992); in Proceedings of the 2nd International Conference on B Physics and CP Violation, Honolulu, Hawaii, 1997, edited by T.E. Browder et al. (World Scientific, Singapore 1998), p. 436
44. CLEO Collaboration, R. Balest et al., Phys. Rev. Lett. **79**, 1436 (1997)
45. X.Q. Li, B. Zou, Phys. Lett. B **399**, 297 (1997)
46. H.Y. Cheng, K.C. Yang, Phys. Rev. D **59**, 092004 (1999)
47. D.S. Du, H. Gong, J. Sung, D. Yang, G. Zhu, hep-ph/0201253
48. Y.Y. Keum, H.n. Li, A.I. Sanda, hep-ph/0201103
49. J.F. Donoghue, E. Golowich, A.A. Petrov, J.M. Soares, Phys. Rev. Lett. **77**, 2178 (1996)
50. B. Blok, I. Halperin, Phys. Lett. **385**, 324 (1996)